Chapter 3

Selectivity for HCO₂⁻ over H₂ in the Electrochemical Catalytic Reduction of CO₂ by (POCOP)Ir(H)₂

With contributions from Robert J. Nielsen and William A. Goddard III

Introduction

A major challenge for society is to develop energy efficient, earth-abundant catalysts that can selectively reduce CO_2 to liquid fuels or other valuable organics[1]. Multiple paths from CO_2 to liquid fuels exist, including chemical (hydrogenation)[2-6] and electrocatalytic (applying a sufficient voltage in a protic medium) routes. Many transition metal electrocatalysts exist to facilitate reactions generating formate or CO[5-8] but for most, product selectivity is an issue.
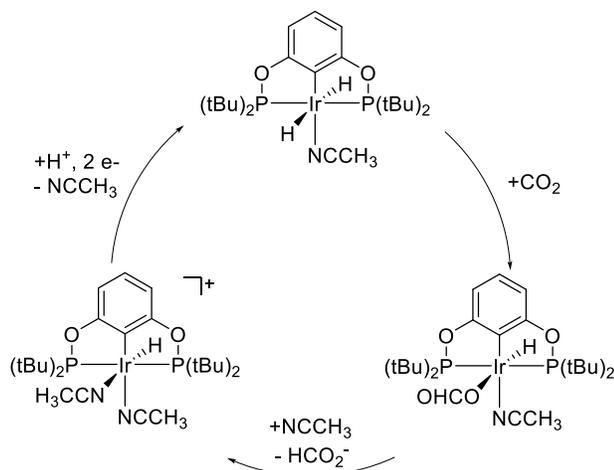
Figure 3.1: Meyer and Brookhart POCOP complex and their proposed mechanism

Among electrocatalysts for the CO_2 reduction reaction (CO_2RR), $[Ru(bpy)_2(CO)_2]^{2+}$ has been shown to reduce CO_2 to CO in acetonitrile and methanol[9]. Rhodium and iridium analogues of this complex have also been developed and shown to electrocatalytically produce formate, though with significant competition from hydrogen evolution.[10] In the case of

$[Rh(bpy)_2(OTf)_2][OTf]$, Faradaic efficiencies for H_2 production ranged between 5 and 20%, decreasing when water was added. Faradaic efficiency refers to the percent of electrons that go to the desired reaction versus an undesired reaction. It is essentially a quantifier for selectivity. Both Kubiak and Sauvage's work with Ni cyclam reducing CO_2 to CO in water and acetonitrile shows that earth abundant metals can serve as electrocatalysts.[11,12] The Ni-cyclam system produced CO with 60% Faradaic efficiency and H_2 at 10% Faradaic efficiency at a potential of -1.61 V. By changing the potential to -1.21 V, the H_2 production was reduced to zero.[11] These systems illustrate the challenge posed by the thermodynamic preference for reduction of protons over CO_2. $(bpy)Re(CO)_3^-$ and $(bpy)Mn(CO)_3^-$ notably reduce CO_2 to CO in the presence of weak acids with limited or no H_2 production.[13,14] Some pincer complexes are also interesting in this regard, including a (PPP)Pd complex studied by Dubois that electrochemically reduced CO_2 to CO, though this was in competition with HER.[15] Berben and coworkers' recent $[Fe_4N(CO)_{12}]^-$ system also displays high selectivity, producing formate with 96% Faradaic yield.[16,17] Understanding of the atomistic origin of selectivity in electrocatalysis is valuable but unclear.

An advance was the (POCOP)Ir catalyst in Figure 3.1, which Meyer and Brookhart showed reduces CO_2 to formate in acetonitrile with 5% water, while wasting only 15% of the current on hydrogen generation. Hydrogen evolution was shown to be a side reaction occurring at the electrode, rather than one directly catalyzed by the metal complex.[18] Furthermore, by adding a quaternary amine functional group to the aryl group of the pincer, they were able to perform electrocatalytic reduction in water with only 5% Faradaic efficiency for H_2 evolution, which again was determined to occur at the electrode.[19,20] Additionally, this catalyst can be noncovalently attached to carbon nanotubes maintaining high TON.[20] The mechanism of the acetonitrile/water system was studied computationally by Cao et al., who implied that regenerating an Ir^{III} dihydride involved reduction of coordinated acetonitrile rather than Ir^{I}.[21] Hazari et al. also explored an alternative mechanism of CO_2 insertion for hydrogenation reactions, coordinating CO_2 to the five-coordinate iridium dihydride complex, as opposed to Cao's hydride transfer to CO_2 from $Ir(H)_2(NCCH_3)$[22]. An alternative mechanism has also been suggested in which CO_2 is primarily reduced by an anionic Ir^{I} hydride rather than the Ir^{III} dihydride.[23]

Toward the goal of understanding this unique catalyst, we report here a series of first principles density functional theory calculations including solvent effects in water to elucidate the mechanism by which CO_2 is reduced by the (POCOP)Ir catalyst. Our proposed mechanism, which relies on CO_2RR via the Ir^{III} hydride, is consistent with all current experiments and the surprising result that only formate is produced without HER. We examine reaction mechanisms with various proton sources leading to hydrogen generation to show that these barriers are high enough that HER is kinetically disfavored. We also investigate whether the cobalt analogue, which has been synthesized previously,[24] can carry out the same chemistry. We find here that the reaction barrier and overpotential are too high and that hydrogen would likely be produced. We conclude by proposing strategies for designing formate-selective CO_2 reduction catalysts, including an analysis of thermodynamic driving forces and the effects of solvation.

Methods

Geometry optimization, frequency, and solvation calculations were performed using the B3LYP hybrid density functional[25,26] with the Los Alamos small core potential[27] and 2-ζ basis set on metals and 6-31G** on organics.[28,29] Single point energies were completed using the M06 functional[30] with LACV3P**++ augmented with f-functions[31] and diffuse functions on cobalt and iridium atoms and the 6-311G**++ basis on organics.[32,33] Solvent effects representing neat water were calculated using an implicit solvation model, using a dielectric constant of 80.37 and a solvent radius of 1.40 Å. To determine accurate free energies for solvent molecules, the 1 atm ideal gas free energy of water was computed using the appropriate statistical mechanics formulae, and the empirical free energies of vaporization (2.05 kcal/mol[34,35] water in water and 2.45 for 1M MeCN in water) were subtracted. The empirical solvation energy of formate in water[36] was used. For hydricity calculations, solvation by acetonitrile was modeled using implicit solvation with a dielectric constant of 37.5 and probe radius of 2.19 Å. Solvation of acetonitrile in acetonitrile was determined from the empirical free energy of vaporization to be 1.27 kcal/mol.[37]

The free energies of organometallic species were calculated using:

$$G = E_{M06} + G_{solv} + E_{ZPE} + H_{vib} + H_{TR} - T(S_{vib} + S_{elec} + S_{TR})$$

where G_{solv} is the free energy of solvation, E_{ZPE} is the zero point energy correction, H_{TR} $(^{12}/_2$ $k_BT)$ is the translational and rotational enthalpy, and S_{vib}, S_{elec}, and S_{TR} are the vibrational, electronic and translational and rotational entropies, respectively. Gas phase translational and rotational entropies were modified by corrections suggested by Wertz.[38] For redox processes, free energies were calculated assuming an operating potential of -1.2V vs NHE. All calculations were completed in Jaguar.[39]

Results and Discussion
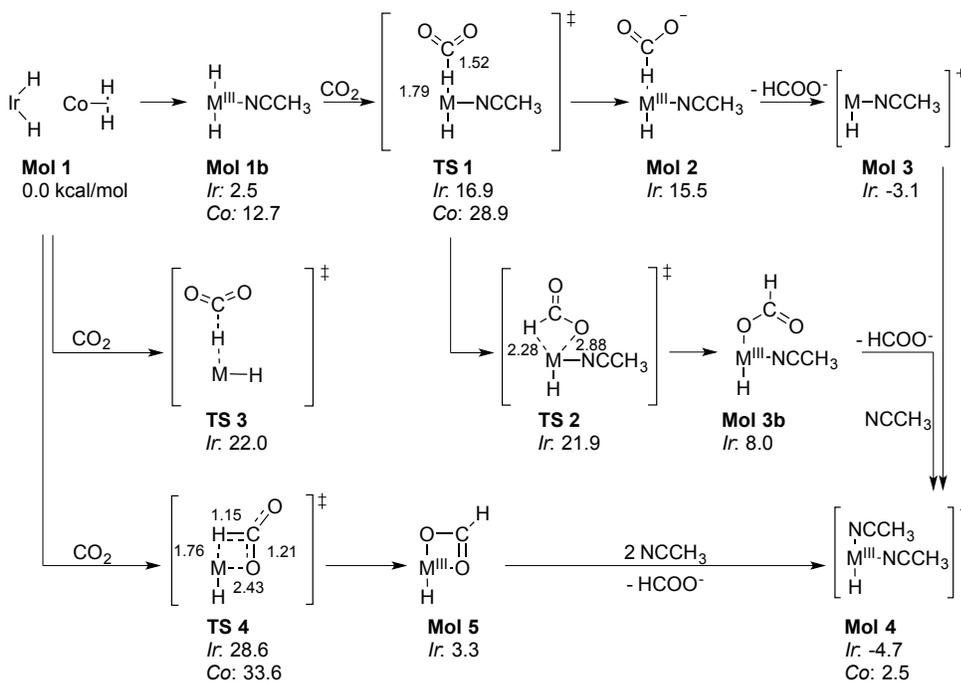
Scheme 3.1: Plausible reaction pathways with calculated free energies (in kcal/mol) and bond lengths (in Ångstroms) for the Ir case.

CO₂ Conversion

Multiple paths for the reaction of (POCOP)Ir(H)$_2$ (**Mol 1**) with CO_2 are shown in Scheme 3.1, along with the calculated free energies including implicit solvation by water. **Mol 1**, the reference state for all calculations, represents the catalyst sans coordinating acetonitrile.[40] Several transition states can be calculated without the presence of acetonitrile. In the lower pathway through **TS 4**, which outlines the mechanism described by Hazari et al.,[22] CO_2 reacts directly with the ground state of the catalyst. In this route, CO_2 can concertedly abstract a hydride and coordinate to the

metal through one of the oxygens at the empty octahedral position. In **Mol 5** the hydride is abstracted and the newly created formate ion is coordinated in κ^2 fashion to the metal. Both κ^1 and κ^2 conformations were calculated, with κ^2 yielding the lowest energy. Formate then dissociates and is replaced by two solvent molecules in **Mol 4**, which then must be reduced to regenerate **Mol 1.** The primary barrier for this process, **TS 4**, is thermally inaccessible at room temperature so this pathway is not likely.

An alternative pathway involves hydride transfer to an uncoordinated CO_2. This can occur directly or after coordination by an acetonitrile as proposed by Cao et al.[21] The coordination of acetonitrile to **Mol 1** to form **Mol 1b** costs 2.5 kcal/mol. We find that constraining the H-Ir-H fragment in **Mol 1** to its linear configuration as in **Mol 1b** requires 19.6 kcal/mol of strain energy, but this is balanced by the binding of acetonitrile. This configuration forces the two hydrides to be *trans* to one another, a configuration that has been shown to be beneficial towards hydride donation[1]. With all octahedral positions filled, CO_2 can abstract a hydride directly, as shown in **TS 1**. In this transition state, the CO_2 has been bent to an angle of 147°, showing that donation of electron density into the π system of CO_2 has occurred. A representation of this transition state can be seen in Figure 3.2a. The barrier for this process is thermally accessible at 16.9 kcal/mol, which is far lower than **TS 4** and matches the activation energy suggested by transition state theory and the turnover frequency of 7.3 s^{-1} derived from cyclic voltammetry (CV) data.[19] Alternatively, the barrier for hydride transfer directly from **Mol 1** to uncoordinated CO_2 is 22.0 kcal/mol, as shown in **TS 3**. In this transition state, the spectator hydride rotates closer to the equatorial position, while the active hydride stays in the axial position to be abstracted by the CO_2, giving a H-Ir-H angle of 89.3°. This represents a large distortion relative to **TS 1** and increases the overall barrier. The alternative transition state wherein CO_2 abstracts equatorial hydride was reported by Osadchuk et al. to have a barrier of 19.0 kcal/mol, which is still higher than those involving coordination of acetonitrile.[23] This demonstrates that by enforcing an octahedral geometry, binding acetonitrile lowers the hydride transfer barrier, explaining the observation that small amounts of acetonitrile must be present for CO_2 reduction to progress.[19] Water is not effective in this role, as it does not allow π−backbonding and coordinates weakly (*vide infra*). In fact the analogue of **TS 1** in which water replaces MeCN poses a barrier of 25.7 kcal/mol. Additionally, work by Ramakrishnan *et al.* suggests that in similar pincer systems, a

π−acidity in the ligand *cis* to the hydride can aid by driving the formation of the formato ligand downhill in energy.[41]

A.

B.
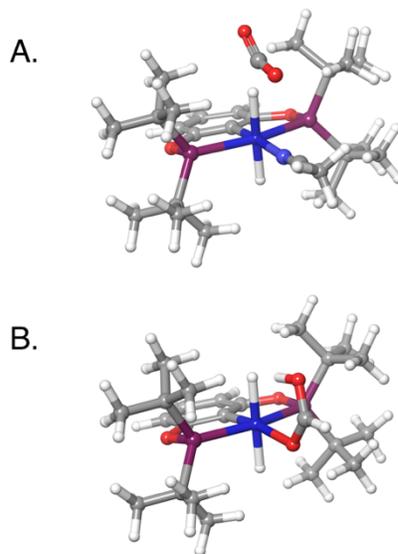
Figure 3.2: Transition states for CO_2RR (A.) and protonation by formic acid (B.).

Following hydride transfer through **TS 1**, a shallow minimum exists, **Mol 2**, in which formate is coordinated through the hydrogen atom. In the mechanism proposed by Cao et al, formate reorients via **TS 2** to coordinate through oxygen, forming intermediate **Mol 3b**. Formate is then released and another solvent molecule coordinates, forming **Mol 4**, which is ready for regeneration. The energy for **TS 2** in iridium is 21.9 kcal/mol, making it difficult to overcome at the experimental temperatures. Instead, formate can simply dissociate, forming **Mol 3.** which is lower in energy than **Mol 3b**, rendering **TS 2** unnecessary. In water, the formate ion can be better solvated, which further favors this pathway as noted by Meyer and coworkers.[19]

The geometries and HOMOs for **Mol 1** can be seen in Figure 3.3. In the iridium compound, the H-Ir-H bond angle is 62° with an H-H distance of 1.62 Å, suggesting the formation of a true dihydride, rather than a dihydrogen adduct. Ir^I is nucleophilic and able to form strong covalent bonds, which encourage the formation of the dihydride.
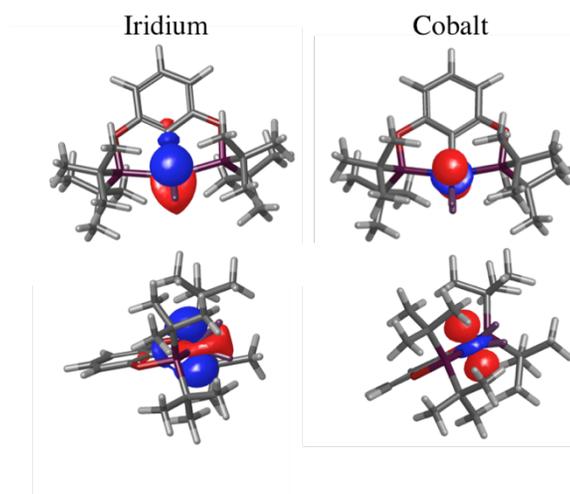
Figure 3.3: The HOMO of **Mol 1** for iridium (left) and cobalt (right), showing the preference in iridium for the formation of the dihydride as opposed to the dihydrogen adduct in cobalt.

Electrochemical Catalyst Regeneration

Since all potential paths yield the Ir^{III} monohydride exergonically, electrochemical regeneration from **Mol 4** is examined in Scheme 3.2. In the net reduction, the two acetonitrile molecules are released and the metal is reduced by two electrons, forming a metal hydride. In this process, the first reduction of **Mol 4** to **Mol 6** is the potential-determining step, as it has a potential of -1.31 V (free energies are calculated at an applied potential of -1.2 V) and requires solvent loss and a change in geometry. This is in agreement with the irreversible reduction potential of -1.3 V vs NHE, measured experimentally by Brookhart et al. for $(POCOP)Ir(H)(NCMe)_2^+$ under argon.[19] This process may be aided by initial dissociation of one acetonitrile molecule (**Mol 3**). The doublet iridium hydride has a bent geometry with a C-Ir-H angle of 143°. The HSOMO is a quasi d-π orbital, shown in Figure 3.4**.** Another electron further reduces the Ir^{II} hydride to a square planar anionic singlet **Mol 7** spontaneously at the operating potential of -1.2 V vs NHE. This further aligns with experimental work by Brookhart et al., as the cyclic voltammetry data obtained for this catalyst indicate an irreversible two electron reduction.[18,19] Finally, exergonic protonation of the metal and coordination of solvent regenerates the original catalyst. This mechanism is in contrast to that of Cao et al., which features a concerted two electron reduction of **Mol 4** to make a compound with a bent acetonitrile ligand.[21] In this case, the acetonitrile has been reduced, rather than the metal center. Examination of this reaction can be seen in Appendix

A.1. The Ir^I product of reduction (**Mol 7**) is 39.0 kcal/mol more stable than Ir^{III} coordinated by a reduced acetonitrile ligand.
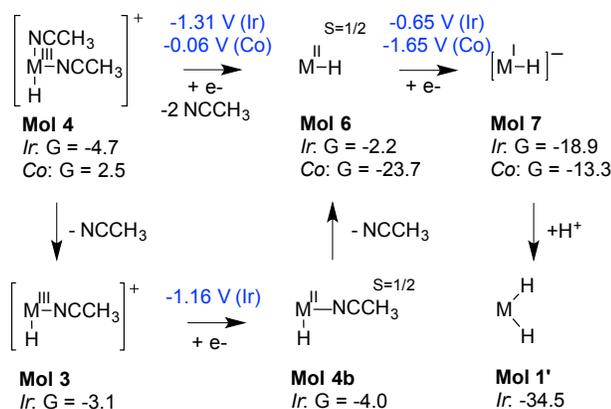
Scheme 3.2: Proposed regeneration of the catalyst occurs as solvent dissociates and the metal is reduced. Free energies (kcal/mol) and potentials (V vs NHE, blue) are reported.
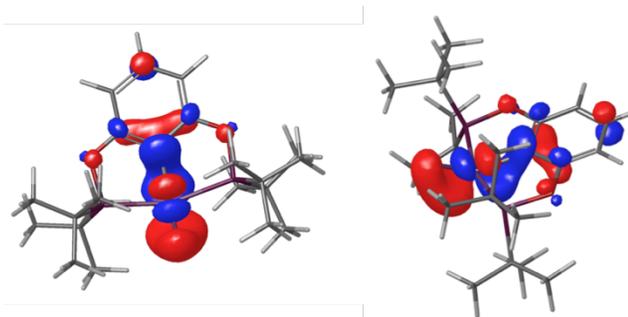
Figure 3.4: The HSOMO of the Ir^{II} hydride complex (**Mol 7**) shows the bent geometry and quasi d-π orbital.

The ability of the iridium hydride anion, **Mol 7,** to reduce CO_2 was also evaluated (Scheme 3.3). In **TS 5**, the CO_2 molecule abstracts the hydride, resulting in coordinated formate, similar to **TS 1**. The hydride abstraction transition state was found to have an energy of -6.5 kcal/mol, or a barrier of 12.4 kcal/mol from the immediately preceding intermediate, slightly lower than that of **TS 1.** We attempted to find a transition state analogous to **TS 4,** but oxygen does not coordinate to the axial positions in this case. The HOMO and HOMO-1 of the molecule (Appendix A.2) explain this behavior, as the oxygen atoms in CO_2 are repelled by the high electron density in the axial positions. This transition state being fully accessible raises the possibility of a secondary catalytic cycle that involves hydride transfer from Ir^I followed by

protonation to generate the Ir^{III} monohydride **Mol 4**, as recently discussed by Osadchuk et al.[23] A secondary cycle has been reported for $(PCNCP)IrH_3$ systems, where both the trihydride and dihydride Ir^{III} complexes are capable of CO_2RR.[42] Additionally, the Ir^I hydride, as well as the ground state, could also be a precursor to hydrogen evolution. To explore potential hydrogen evolution reactions and CO_2RR from the Ir^I hydride, a look into the kinetics of proton transfer reactions is necessary.
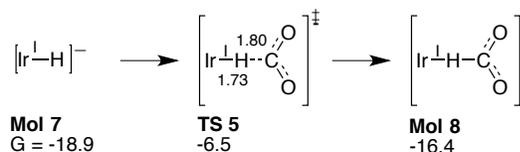
Scheme 3.3: Reaction of the iridium hydride anion with CO_2 is thermodynamically feasible, but is competitive with protonation. Free energies are reported in kcal/mol.

Hydrogen Evolution

It is remarkable that this catalyst is selective for formate generation over hydrogen evolution in water, even though both Ir^{III} dihydride and Ir^I hydride are intermediates from which an HER mechanism could branch. In the case of the Ir^{III} dihydride complex, looking only at the thermodynamics of intermediates (Scheme 3.4), it would appear that hydrogen evolution is feasible, as all energies are thermally accessible. This implies that the impediment to hydrogen evolution is the reactivity of metal hydrides, not their formation, as has been found in other systems.[43] In work by Kang et al., it was suggested that the preference for dihydride (over dihydrogen adduct) was the source of this selectivity.[20]
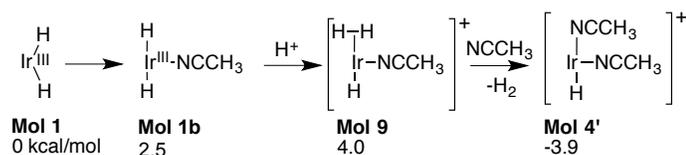
Scheme 3.4: Free energies illustrating the thermodynamic, but not kinetic, feasibility of hydrogen evolution.

If HER is not thermodynamically prohibited, it may be limited by kinetics. In order to explore kinetics, potential routes for hydrogen evolution are considered in Schemes 3.5-3.7. Scheme 3.5

shows protonation of the hydride by an external water cluster, which then proceeds to **Mol 9**, the dihydrogen complex. The shapes of the water clusters were chosen to maximize solvation of the water donating a proton. The two geometries included a square water cluster, (Cluster 1), and a Y-shaped cluster (Cluster 2.) Multi-water clusters have been used in CO_2 reduction and other organometallic studies[44,45], and we find the cluster, combined with implicit solvation, accurately reproduces the pKa's of water (Appendix A.3). The water cluster was present for both the ground state and the transition states, ensuring that when comparing barrier heights, the energy of forming the water cluster does not affect the results. In this reaction, Cluster 1 is unstable and quickly relaxes to Cluster 2. This may be due to the steric effect of the t-butyl groups. The activation energy of 27.0 kcal/mol for Cluster 2 is much higher than the competing CO_2RR pathway (**TS 1**). While **Mol 9** appears to be thermodynamically accessible, the path through external protonation by weak acids is not.
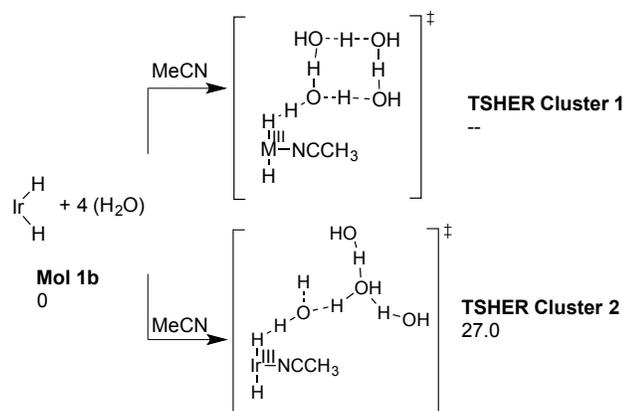
Scheme 3.5: Free energies of protonation of the dihydride by different water cluster geometries

In Scheme 3.6, the intramolecular reaction between coordinated water and hydride can be seen. The complex **Mol 1** first undergoes coordination by water to form **Mol 10**. This is unfavorable, especially relative to coordination by acetonitrile: the t-butyl groups create a hydrophobic pocket, and the lack of π-acidity in water removes back bonding between water and the metal. The Ir-OH_2 distance in **Mol 15** (2.33 Å) is much longer than the Ir-N distance in **Mol 1** (2.11 Å). The preference for acetonitrile is also seen experimentally.[20] Coordinated water then transfers a proton to the hydride. Three configurations for this have been considered, each with increasing number of bridging water molecules to relieve strain. Note that the competing activation barrier

for reacting with CO_2, **TS 1,** is 16.9 kcal/mol. In the case without bridging waters, **TS 6**, the barrier is 28.7 kcal/mol, which is too high to be competitive with CO_2 reduction. Adding one bridging water (**TS 7**) lowers the calculated barrier to 27.2 kcal/mol, while adding a second bridging water (**TS 8**) increases the barrier. This signifies that adding water molecules does not significantly decrease the calculated barrier. This route also does not appear to be possible.
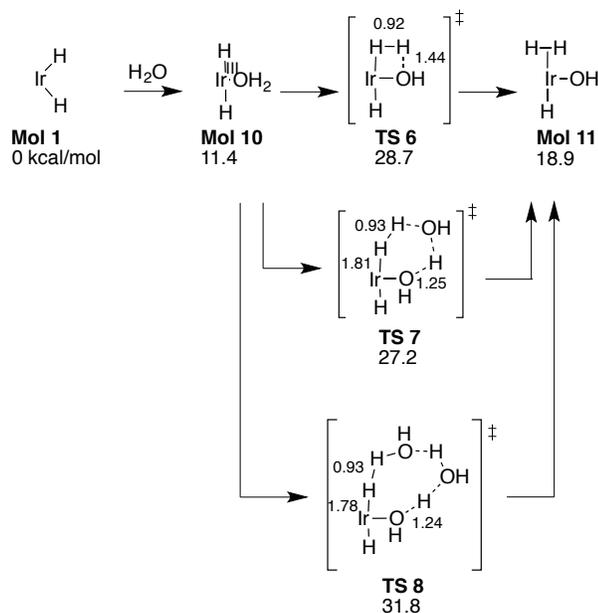
Scheme 3.6: Intramolecular protonation of the dihydride. Bridging waters lower the barrier, but this path is not competitive with CO_2 reduction. Free energies are reported.

It is worth noting the entropies of activation for **Mol 1b** + CO_2 (0.035M) → **TS 1** for CO_2 reduction and **Mol 1b** → **TSHER Cluster 2** for internal protonation leading to HER are -20.3 cal/mol·K (using the calculated $\Delta S^{\ddagger}_{vib}$, ΔS_{CO2}(1atm→1M,aq) = -23.0 cal/mol·K[46] and 0.035 M for the concentration of CO_2 in water[47]) and -4.5 cal/mol·K, respectively. Selectivity towards CO_2 reduction therefore benefits from the low temperature of the reaction.
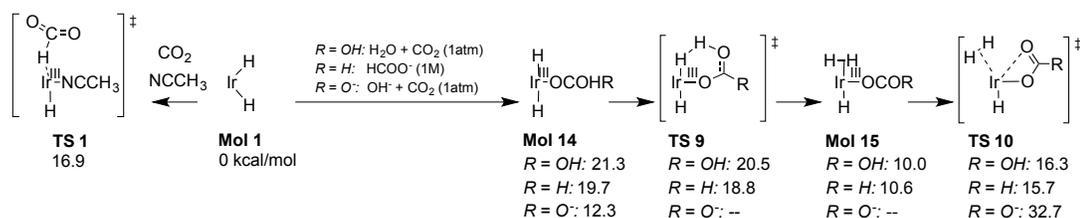
Scheme 3.7: Free energies for potential pathways for the formation of hydrogen involving carbonic acid, formic acid, and bicarbonate in water, pH = 7

In addition to water, other proton sources generated in reaction conditions could be involved in HER. Formic acid, bicarbonate, or carbonic acid formed *in situ*, with pK_A's nearer the reaction conditions than H_3O^+ or H_2O, could catalyze HER. In order to explore these possibilities, the paths for proton transfer from these three species are compared in Scheme 3.7. First, the proton source coordinates to form **Mol 14.** It is important that for all species, as with water, this is unfavorable. From **Mol 14**, a proton is then transferred from the bound acid to the hydride (**TS 9**), forming a dihydrogen adduct (**Mol 15**).[48] Dihydrogen dissociates and is replaced by the chelating carboxylate in **TS 10**. In the case of bicarbonate, no stable hydrogen adduct could be located, suggesting that the proton transfer and dihydrogen release are one concerted reaction. The barriers for HER are higher in free energy than hydride transfer to CO_2 in water (16.9 kcal/mol), although the activation barriers *following* coordination of the acid are very low. However, in equilibrium with one atmosphere CO_2 and at the turnover numbers reported, these species would be present in concentrations $\leq 0.1M$. This highlights the importance of reaction conditions on product selectivity, as it appears that as more carboxylates accumulate, these reactions may become competitive with CO_2RR.
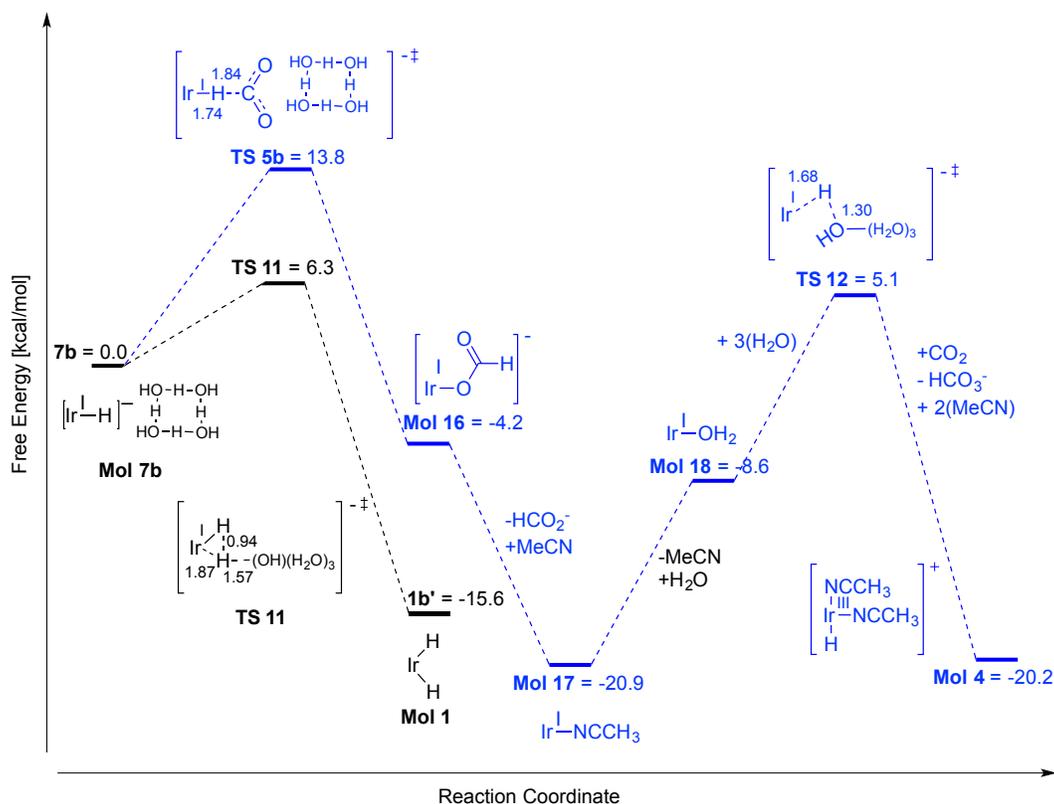
Scheme 3.8: Competing regeneration and CO_2RR routes from the Ir^I hydride anion with the preferred pathway in black. Free energies are reported.

The Ir^I hydride anion **Mol 7** is another potential precursor for both hydrogen evolution and CO_2 reduction.[23] From this intermediate, protonation could lead to formation of a dihydrogen adduct and with the simultaneous coordination of solvent, H_2 can be liberated. However, both from experiment and calculations it can be concluded that this does not occur. Rather than making and H_2 adduct, protonation could also yield the Ir^{III} dihydride **Mol 1**, completing the catalytic cycle. On the other hand, the Ir^I hydride could reduce CO_2, beginning an alternative cycle. In Scheme 3.8, these paths are compared. The thermodynamic reference state is **Mol 7** (for intermediates) or **Mol 7b,** which is **Mol 7** with a four-water cluster present (for transition states that include a four-H_2O cluster).

The lowest barrier found for protonating the monohydride is via **TS 11**, with a 6.3 kcal/mol activation barrier for proton transfer with respect to **Mol 7b** in water. The geometry of **TS 11** is interesting, as the incoming proton appears to bond simultaneously with the hydride and the

metal. Bond lengths from the proton to the hydride and the proton to the metal are 0.94 Å and 1.87 Å, respectively. For reference, in **Mol 7b**, the Ir hydride bond length is 1.71 Å. This suggests a late transition state that leads to protonation of the metal and regeneration of **Mol 1**. No dihydrogen adduct was located. That **TS 11** leads to the dihydride was confirmed by intrinsic reaction coordinate (IRC) calculations. Figures along this pathway can be seen in Appendix A.6. The equilibrium between dihydride and dihydrogen has been seen in other organometallic compounds[49-51], with certain Fe compounds similarly preferring dihydride formation[52]. A transition state utilizing the Y-shaped cluster can be seen in the Appendix A.5 of the Supporting Information, with a higher barrier of 12.8 kcal/mol. An additional structure with a higher energy of 14.0 kcal/mol was reported by Osadchuk et al. in which the Ir atom is directly protonated at the axial position.[23] We could not identify a saddle point on the potential energy surface (in vacuum or including continuum solvation) with this geometry. The lower barrier of the hydridic protonation path **TS 11** is in agreement with other inorganic[51], biological,[53,54] and heterogeneous[44] examples demonstrating that direct protonation at the metal is often difficult.

The route in blue shows the path in which the Ir^I-H anion is the active state for CO_2RR. The initial transition state **TS 5b**, the reduction of CO_2 by the metal hydride, has a higher barrier than protonation in the presence of the cluster, implying that protonation will dominate. Without the water cluster included for consistency in **TS 5b**, the activation energy of **TS 5** is 12.4 kcal/mol. Osadchuk et al. identified several routes by which the Ir^{III} complex can be regenerated via protonation by a water cluster. They found feasible barriers from the Ir^I aquo complex, **Mol 18**. However, we find that coordination of acetonitrile to Ir^I, neglected in Reference [23], forms the thermodynamic sink **Mol 17**. The formation of **Mol 17** is 12.3 kcal/mol more exergonic than the aquo complex, implying that this would be the ground state of the alternative, Ir^I-based catalytic cycle. This makes the overall barrier for regeneration via **TS 12** 26.0 kcal/mol, higher than any barrier in the Ir^{III}-based cycle. Additionally one would expect to see this complex in the NMR, but only **Mol 4** is reported.[18,19] While this cycle may operate as a side reaction, the low energies of **TS 11** and **Mol 17** lead us to conclude the majority of CO_2RR in water results from the Ir^{III} dihydride, in agreement with the mechanism proposed by Meyer and Brookhart.[18,19] Experimental clarification of this Ir^{III}/Ir^I dilemma raised by DFT calculations will have

important implications for arguments regarding the design of selective CO_2RR catalysts (*vide infra*).

Cobalt Analogue

In the interest of using earth-abundant metals, we replaced iridium with cobalt and evaluated the same mechanistic pathway. As shown in Scheme 3.1, cobalt prefers to dissociate solvent to form a cobalt dihydrogen complex (**Mol 1**), unlike iridium. The predicted dihydrogen adduct geometry is shown in Figure 3.3. The H-H bond length in the cobalt complex is 0.86 Å, indicative of a dihydrogen bond. In the iridium complex, the H-H distance is 1.66 Å. This is a consequence of the first row metals forming weaker covalent bonds. The result is that **Mol 1** is the more stable state preceding hydride transfer for the cobalt catalyst. This is problematic as it results in both transition states for hydride transfer to CO_2 (**TS 1** and **TS 4**) being thermally inaccessible.

The regeneration pathway for the cobalt case is also unfavorable. As shown in Scheme 3.2, the cobalt catalyst has the behavior opposite of iridium in that the first reduction to the Co^{II} complex, **Mol 6**, is facile, with a potential of -0.06 V vs NHE. However, the second reduction to Co^I at -1.65 V vs NHE is too negative to be practical. The first reduction to Co^{II} involves the loss of two solvent molecules. Previous work has shown that large *t*-butyl groups in the wings of the pincer can sterically destabilize an octahedral complex, encouraging the formation of square planar complexes in iridium pincer complexes.[55] Using a smaller metal like cobalt will enhance this effect, raising the potential for reduction to the square planar cobalt analogue of **Mol 6.** The reduction to Co^I is more difficult, however, than the analogous reduction to Ir^I. The C-M and M-H covalent bonds must be made and orthogonalized by hybridizing s and d_σ orbitals. This is not favorable for Co for which the 3d orbitals are much smaller than the 4s (in contrast the 5d and 6s orbitals have similar size).[56] These difficulties suggest that (POCOP)Co will not function as a CO_2RR electrocatalyst.

Hydricities as a Guiding Design Principle

The hydricities of H_2, formate and the various hydrides discussed above are useful for illustrating the effect of reaction conditions on reaction thermochemistry. Much work has been done to

measure hydricities of CO_2RR and HER catalysts in different solvents[16,57,58] and with different coordinating ions and ligand modifications[15,59-63], to which modeling can add additional understanding. Here we reference driving forces for hydride transfer to the H_2/H^+ couple, eschewing the poorly-characterized hydride ion commonly used to define hydricities (Figure 3.5). Our calculated driving forces can be converted to the traditional hydricities by adding ΔG for $H_2(1atm) \rightarrow H^-(1M) + H^+$ in the conditions of interest. This value varies among references, but at pH = 0 we adopt 76.6 kcal/mol in acetonitrile[64] and 34.2 kcal/mol in water, recently recommended by Appel et al.[65] In water, we discuss values both at the standard 1M H^+ and at pH=7, representative of the experimental conditions. Solvation of a proton in acetonitrile is calculated using from Tissandier's proton solvation energy in water[66] and adding the free energy of solvent transfer recommended by Pegis et al.[67] The hydricity of formate in acetonitrile is from Dubois et al.[62] and in water was calculated using free energies of formation: $HCOO^-(1M) + H^+(1M) \rightarrow CO_2(1atm) + H_2 (1atm)$, ΔG = -10.3 kcal/mol.[46]

The driving force for the iridium dihydride complex in neat acetonitrile is -31.5 kcal/mol. This is insufficient to reduce CO_2, given the driving force (-33 kcal/mol) of formate in neat acetonitrile. However, in water the formate ion is stabilized[68], effectively raising its hydricity about 6 kcal/mol above that of **Mol 1**. Operating at pH 7 rather than the standard state of pH 0 further reduces the tendency toward proton reduction. These values can be seen graphically in Figure 3.5, which shows the same narrowing of hydricity ranges shown in other multi-solvent studies.[57,59]

$Ir(H)_2(NCMe) + H^+(1M) + MeCN(l) \rightarrow Ir(H)(NCMe)_2^+ + H_2(1atm)$
$MeCN(neat)$: $\Delta G_{Hyd} = -31.5$ kcal/mol

$Ir(H)_2(MeCN)$ / $Ir(H)^+(MeCN)_2$ $Ir(H)^-$ / $Ir(MeCN)$

H_2/H^+ $HCOO^-$/CO_2 $Co(H)^-$/$Co(MeCN)$

0   -31.5 -33 -42.3 -51.3   *Hydricities in neat MeCN*

0   -10.3 -16.4 -29.6 -39.5   *Hydricities in water, pH = 0*

-0.8 -6.9 -20.1 -30.0   *Hydricities in water, pH = 7*

$Ir(H)_2(NCMe) + H^+ + MeCN(1\%) \rightarrow Ir(H)(NCMe)_2^+ + H_2(1atm)$
$H_2O (pH=0)$: $\Delta G_{Hyd} = -16.4$ kcal/mol
$H_2O (pH=7)$: $\Delta G_{Hyd} = -6.9$ kcal/mol
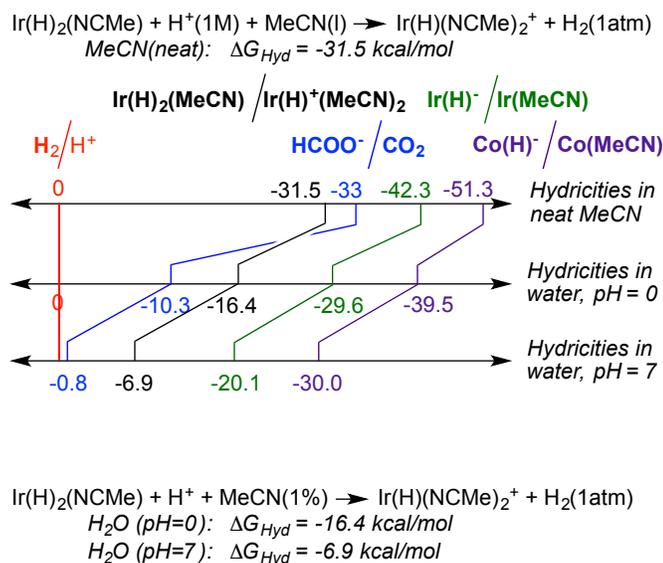
Figure 3.5: Thermodynamic cycle used for calculating the hydricity of the iridium dihydride, hydride, and cobalt hydride in neat acetonitrile and water

Calculated solvation energies shed further light on solvent effects. Table 3.1 provides the difference between the solvation energies of hydride donors and their conjugate Lewis acids. Entries 1-3 show that stabilization of the organometallic cations generated by hydride transfer is roughly equal in both solvents. Also, solvation does not drive the coordination of acetonitrile ligands. Kang et al.[19] added a quaternary amine solvation handle to the (POCOP^{tBu2}) ligand to facilitate catalysis in water. These complexes, denoted with the superscript "quat", can be seen in Appendix A.4. Generation of the dicationic **Mol4^{quat}** is stabilized by solvation more so than monocationic **Mol4**, but again the effect is similar in both solvents.

Table 3.1: *Contribution of solvation free energy (kcal/mol) to hydride transfer reactions.*

I / J	$\Delta G_{solv,J} - \Delta G_{solv,I}$, MeCN	$\Delta G_{solv,J} - \Delta G_{solv,I}$, Water
(Mol 1b + MeCN) / Mol 4	-25.0	-25.6
Mol 1b / Mol 3	-23.0	-27.7
(Mol1 + 2MeCN) / Mol4	-28.9	-26.3
(Mol1b^{quat} + MeCN) / Mol4^{quat}	-68.1	-67.7
Mol1b^{quat} / Mol3^{quat}	-69.5	-68.4
CH₃COO⁻ / CO₂ (1 atm)	58.8[a]	77.6[a]
HCOO⁻ / CO₂ (1 atm)	64.2	77.7

[a]Reference 71

Empirical solvation energies for formate in both solvents were not found, so computed values were used and solvation energies of acetate were used for qualitative comparison. The effect of the solvent on hydricities is clearly not due to solvation of the Ir complexes, but to changes in solvation of formate. By comparison, the empirical solvation energies of a similar ion, acetate, in acetonitrile and water differ by 18.8 kcal/mol.[69] This implies that while the coordinating solvent can decrease the hydricity, the stronger hydride donating force comes largely from the stabilization of the formate ion in water versus acetonitrile rather than a solvation effect on the metal complex. Thus, the presence of water will drive formate production forward through stabilization of the product, as noted by Meyer et al.[18]

Two hydricity-based stategies may be proposed for rational design of formate-selective catalysts. One is to overshoot the hydricity of the CO_2/HCO_2^- couple to accelerate CO_2RR. This approach is illustrated by the potential Ir^I and Co^I-based cycles, as both monohydrides are stronger hydride donors than formate by 20 or 30 kcal/mol in water. In its favor, the Ir^I cycle features a low activation barrier for hydride transfer to CO_2, the same moderate overpotential as the Ir^{III} cycle, and no competing route to hydrogen evolution. The motif that allows this cycle to avoid HER is the basic lone-pair of Ir^I, since protonating this lone pair to generate the dihydride is favorable relative to making a H-H bond. While effective, this motif is generally correlated to (a) a lower reduction potential earlier in the catalytic cycle and (b) a stronger covalent contribution to M-H bonding, and therefore loosely correlated to the abundance of the metal. The iridium metal center is reducing enough to break the putative dihydrogen adduct into the dihydride, and still deliver H^- from Ir^{III} to CO_2. The Co^I analogue supports this interpretation. The reactive hydride shows a strong driving force for reacting with neutral water but is not basic enough to break the H-H bond. Thus, the dihydrogen adduct easily forms and hydrogen evolution is predicted. Creutz et al. measured the rates with which ruthenium hydrides reacted with hydronium and CO_2 in water.[45] The decreased hydricity of $(tpy)(bpy)RuH^+$ relative to $(C_6Me_6)(bpy)RuH^+$ by 9 kcal/mol led to an acceleration of both reactions approximately a thousandfold, supporting no hope for accelerating CO_2 reduction *relative* to HER.

A second strategy is to design the catalyst and conditions to be in a range just hydridic enough to reduce CO_2, while minimizing the rate of hydrogen evolution[8,17] The weaker hydricity of the Ir^{III} dihydride puts it in this range. Additionally, the basic metal center ensures the breakup of

any potential dihydrogen adduct. The activation parameters computed for hydride transfer from the Ir^I hydride (**Mol 7**) and the Ir^{III} dihydride (**Mol 1**) support this strategy. Although the Ir^I hydride offers 13 kcal/mol more driving force to this reaction, the activation free energy is only 3 kcal/mol lower. The activation *enthalpies* (7.8 kcal/mol for Ir^I, 8.4 for Ir^{III}, calculated from aqueous CO_2) are almost equal. The reaction with Ir^I has an earlier transition state. As a guiding principal, choosing the most hydridic catalyst does not ensure selective CO_2RR. The same view has been reached by Taheri and Berben by studying the behavior of $[HFe_4N(CO)_{12}]^-$ and $[HFe_4C(CO)_{12}]^{2-}$. The carbide provides more driving force for hydride transfer and reduces only protons in the presence of CO_2, while the nitride with a moderate hydricity of 15 in water catalyzes CO_2 reduction selectively.[17]

Hydricity calculations alone predict the Ir^{III} dihydride to be competent for hydrogen evolution, though we have shown that the kinetics of the system slow HER relative to CO_2RR in a variety of ways. Just as HER kinetics are not fixed by ΔG_{H^-}, so CO_2RR kinetics may not be either. As hydricities are purely thermodynamic quantities, they may not capture subtleties in the system such as hydrogen bonding, steric crowding, or hydrophobic pockets which may affect a transition state barrier. The hydricity of the Ir^{III} dihydride can be compared to other complexes with measured hydricities, as shown in Appendix A.7. Dubois and coworkers[15,60] found that plotting the first reduction potential of (P_4)Ni and Pd complexes against their measured hydricities displayed a linear correlation, with more hydridic complexes also having a more negative first reduction potential. While (POCOP)Ir's hydricity is similar to the more hydritic Ni and Pd complexes, a more negative first reduction potential is required to achieve it. As a 3rd row metal, Ir makes a very strong metal-hydride covalent bond and prefers not to undergo an odd-electron reduction, making this first reduction more difficult. This implies that more energy is required to achieve the hydricity in (POCOP)Ir compared to the 1st and 2nd row metals in standard ligand sets and that this behavior may be typical of other 3rd row metals.

Conclusions

(POCOP)Ir presents an interesting case of a selective CO_2RR catalyst that efficiently produces formate in the presence of water without evolving hydrogen. The iridium-based catalyst is shown through a mechanistic study to have an accessible barrier for CO_2 reduction (via hydride transfer

from a six-coordinate dihydride) and is able to be electrocatalytically regenerated through an Ir^{I} hydride intermediate (-1.31 V vs NHE calculated for the one-electron reduction of $(POCOP)Ir^{III}(H)(MeCN)_2^+$). In the cobalt analogue, both CO_2 reduction ($\Delta G^{\ddagger} = 28.9$ kcal/mol) and electrochemical regeneration are prohibited (-1.65 V vs NHE calculated for the one-electron reduction of $(POCOP)Co^{II}(H)$) under mild conditions. $(POCOP)Co$ also prefers the formation of a dihydrogen adduct, in contrast to Ir, which prefers the formation of the dihydride.

Hydrogen evolution via protonation of Ir^{III} and Ir^{I} hydrides by water, is prohibited by high activation barriers (in excess of 25 kcal/mol). HER barriers within 2 kcal/mol of the CO2RR barrier are predicted if catalyzed by molar concentrations of carboxylates. A number of factors cooperate to promote selectivity for CO_2 reduction over the thermodynamically favored reduction of protons. Generically, the neutral-pH, aqueous solvent minimizes the disparity between the driving forces for two-electron reductions of protons and CO_2. $H_2(g) + CO_2(g) \rightarrow HCO_2^-(1M) + H^+$ is only one kcal/mol uphill in water at pH = 7.[46] Since the entropy of activation for hydride transfer to CO_2 is more negative than that for reduction of water, selectivity also benefits from the mild, ambient temperature of the reaction. The binding of acetonitrile to the $(POCOP)IrH_2$ species simultaneously *promotes* hydride transfer to CO_2 and *inhibits* intramolecular pathways by which water and carboxylates can catalyze HER. The low concentration of carboxylates, which can act as 2nd coordination sphere proton relays, also raises these barriers for HER. In both the transition states for hydride transfer to CO_2 and to uncoordinated water, the iridium-hydride covalent bond is broken and replaced with an H-C or H-H sigma-adduct. However, only the latter reaction requires a strong bond (H-OH) to be broken simultaneously. Significant barriers for proton transfer from weak acids to reduced metals similarly promote selectivity toward the reduction of CO_2 to CO by catalysts whose metals bind CO_2 directly[14,43,70]. The basicity of the Ir^{I} center encourages protonation to occur leading to the formation of an additional strong Ir-H bond rather than the evolution of H_2. Protonolysis of Ir^{I}-hydride bonds to generate H_2 is also kinetically unfavorable. These results suggest that a moderate hydricity is key in selective CO_2 reduction to formate.

References

(1) Schmeier, T. J.; Dobereiner, G. E.; Crabtree, R. H.; Hazari, N. *J. Am. Chem. Soc.* **2011**, *133*, 9274-9277.

(2) Kaska, W. C.; Nemeh, S.; Shirazi, A.; Potuznik, S. *Organomet.* **1988**, *7*, 13-15.

(3) Langer, R.; Diskin-Posner, Y.; Leitus, G.; Shimon, L. J. W.; Ben-David, Y.; Milstein, D. *Angew. Chem. Int. Ed.* **2011**, *50*, 9948-9952.

(4) Ahlquist, M. S. G. *J. Mol. Cat. A: Chem.* **2010**, *324*, 3-8.

(5) Jessop, P. G.; Joó, F.; Tai, C.-C. *Coord. Chem. Rev.* **2004**, *248*, 2425-2442.

(6) Benson, E. E.; Kubiak, C. P.; Sathrum, A. J.; Smieja, J. M. *Chem. Soc. Rev.* **2009**, *38*, 89-99.

(7) Costentin, C.; Robert, M.; Saveant, J.-M. *Chem. Soc. Rev.* **2013**, *42*, 2423-2436.

(8) Taheri, A.; Berben, L. A. *Chem. Comm.* **2016**, *52*, 1768-1777.

(9) Ishida, H.; Tanaka, H.; Tanaka, K.; Tanaka, T. *Chem. Commun.* **1987**, 131-132.

(10) Bolinger, C. M.; Story, N.; Sullivan, B. P.; Meyer, T. J. *Inorg. Chem.* **1988**, *27*, 4582-4587.

(11) Froehlich, J. D.; Kubiak, C. P. *Inorg. Chem.* **2012**, *51*, 3932-3934.

(12) Beley, M.; Collin, J. P.; Ruppert, R.; Sauvage, J. P. *Chem. Commun.* **1984**, 1315-1316.

(13) Hawecker, J.; Lehn, J. M.; Ziessel, R. *Chem. Commun.* **1984**, 328-330.

(14) Smieja, J. M.; Sampson, M. D.; Grice, K. A.; Benson, E. E.; Froehlich, J. D.; Kubiak, C. P. *Inorg. Chem.* **2013**, *52*, 2484-2491.

(15) Dubois, D. L.; Miedaner, A.; Haltiwanger, R. C. *J. Am. Chem. Soc.* **1991**, *113*, 8753-8764.

(16) Taheri, A.; Thompson, E. J.; Fettinger, J. C.; Berben, L. A. *ACS Catal.* **2015**, *5*, 7140-7151.

(17) Taheri, A.; Berben, L. A. *Inorg. Chem.* **2016**, *55*, 378-385.

(18) Kang, P.; Cheng, C.; Chen, Z.; Schauer, C. K.; Meyer, T. J.; Brookhart, M. *J. Am. Chem. Soc.* **2012**, *134*, 5500-5503.

(19) Kang, P.; Meyer, T. J.; Brookhart, M. *Chem. Sci.* **2013**, *4*, 3497-3502.

(20) Kang, P.; Chen, Z.; Brookhart, M.; Meyer, T. *Top. Catal.* **2014**, *58*, 30-45.

(21) Cao, L.; Sun, C.; Sun, N.; Meng, L.; Chen, D. *Dalton Trans.* **2013**, *42*, 5755-5763.

(22) Bernskoetter, W. H.; Hazari, N. *Eur. J. Inorg. Chem.* **2013**, 4032-4041.

(23) Osadchuk, I.; Tamm, T.; Ahlquist, M. S. G. *ACS Catal.* **2016**, 3834-3839.

(24) Hebden, T. J.; St. John, A. J.; Gusev, D. G.; Kaminsky, W.; Goldberg, K. I.; Heinekey, D. M. *Angew. Chem. Int. Ed.* **2011**, *50*, 1873-1876.

(25) Becke, A. D. *J. Chem. Phys.* **1993**, *98*, 5648-5652.

(26) Lee, C. T.; Yang, W. T.; Parr, R. G. *Phys. Rev. B* **1988**, *37*, 785-789.

(27) Hay, P. J.; Wadt, W. R. *J. Chem. Phys.* **1985**, *82*, 299-310.

(28) Francl, M. M.; Pietro, W. J.; Hehre, W. J.; Binkley, J. S.; Gordon, M. S.; Defrees, D. J.; Pople, J. A. *J. Chem. Phys.* **1982**, *77*, 3654-3665.

(29) Hehre, W. J.; Ditchfie.R; Pople, J. A. *J. Chem. Phys.* **1972**, *56*, 2257-2261.

(30) Zhao, Y.; Truhlar, D. G. *Theor. Chem. Acc.* **2008**, *120*, 215-241.

(31) Martin, J. M. L.; Sundermann, A. *J. Chem. Phys.* **2001**, *114*, 3408-3420.

(32) Clark, T.; Chandrasekhar, J.; Spitznagel, G. W.; Schleyer, P. V. *J. Comp. Chem.* **1983**, *4*, 294-301.

(33) Krishnan, R.; Binkley, J. S.; Seeger, R.; Pople, J. A. *J. Chem. Phys.* **1980**, *72*, 650-654.

(34) Dojcansky, J.; Heinrich, J. *Chem. Zvesti* **1974**, *28*, 157-159.

(35) Putnam, W. E.; McEachern, D. M. J.; Kilpatrick, J. E. *J. Chem. Phys.* **1965**, *42*, 749-755.

(36) Kelly, C. P.; Cramer, C. J.; Truhlar, D. G. *J. Phys. Chem. B* **2006**, *110*, 16066-16081.

(37) Bridgeman, O. C., Aldrich, E.W., *J. Heat Transfer* **1964**, *86*, 279-286.

(38) Wertz, D. H. *J. Am. Chem. Soc.* **1980**, *102*, 5316-5322.

(39) Bochevarov, A. D.; Harder, E.; Hughes, T. F.; Greenwood, J. R.; Braden, D. A.; Philipp, D. M.; Rinaldo, D.; Halls, M. D.; Zhang, J.; Friesner, R. A. *Int. J. Quantum Chem.* **2013**, *113*, 2110-2142.

(40) While other work has posited that five-coordinate (POCOP)Ir(H)2 can oscillate between Y-shaped (distorted trigonal bipyrimidal) and T-shaped (square pyramidal) depending on solvent conditions (see refs. 40 and 41), the reported geometry is Y-shaped, which was confirmed using large basis set calculations in solvent.

(41) Ramakrishnan, S.; Waldie, K. M.; Warnke, I.; De Crisci, A. G.; Batista, V. S.; Waymouth, R. M.; Chidsey, C. E. D. *Inorg. Chem.* **2016**, *55*, 1623-1632.

(42) Osadchuk, I.; Tamm, T.; Ahlquist, M. S. G. *Organometallics* **2015**, *34*, 4932-4940.

(43) Keith, J. A.; Grice, K. A.; Kubiak, C. P.; Carter, E. A. *J. Am. Chem. Soc.* **2013**, *135*, 15823-15829.

(44) Huang, Y.; Nielsen, R. J.; Goddard, W. A.; Soriaga, M. P. *J. Am. Chem. Soc.* **2015**, *137*, 6692-6698.

(45) Creutz, C.; Chou, M. H.; Hou, H.; Muckerman, J. T. *Inorg. Chem.* **2010**, *49*, 9809-9822.

(46) Wagman, D. D.; Evans, W. H.; Parker, V. B.; Schumm, R. H.; Halow, I. *The NBS tables of chemical thermodynamic properties. Selected values for inorganic and C1 and C2 organic substances in SI units*, National Standard Reference Data System, 1982.

(47) Morrison, T. J.; Billett, F. *J. Chem Soc.* **1952**, 3819-3822.

(48) In the case of R = OH, Mol 12 is a shallow minimum on the potential energy surface, but due to the loss of the zero point energy of the OH bond, it is higher in free energy than the subsequent transition state, TS 4. This effectively makes the energy of Mol 12 the barrier in this process.

(49) Albinati, A.; Bakhmutov, V. I.; Belkova, N. V.; Bianchini, C.; de los Rios, I.; Epstein, L.; Gutsul, E. I.; Marvelli, L.; Peruzzini, M.; Rossi, R.; Shubina, E.; Vorontsov, E. V.; Zanobini, F. *Eur. J. Inorg. Chem.* **2002**, 1530-1539.

(50) Belkova, N. V.; Collange, E.; Dub, P.; Epstein, L. M.; Lemenovskii, D. A.; Lledos, A.; Maresca, O.; Maseras, F.; Poli, R.; Revin, P. O.; Shubina, E. S.; Vorontsov, E. V. *Chem. Eur. J.* **2005**, *11*, 873-888.

(51) Besora, M.; Lledos, A.; Maseras, F. *Chem. Soc. Rev.* **2009**, *38*, 957-966.

(52) Baya, M.; Maresca, O.; Poli, R.; Coppel, Y.; Maseras, F.; Lledos, A.; Belkova, N. V.; Dub, P. A.; Epstein, L. M.; Shubina, E. S. *Inorg. Chem.* **2006**, *45*, 10248-10262.

(53) Eilers, G.; Schwartz, L.; Stein, M.; Zampella, G.; de Gioia, L.; Ott, S.; Lomoth, R. *Chem. Eur. J.* **2007**, *13*, 7075-7084.

(54) Carroll, M. E.; Barton, B. E.; Rauchfuss, T. B.; Carroll, P. J. *J. Am. Chem. Soc.* **2012**, *134*, 18843-18852.

(55) Lokare, K. S.; Nielsen, R. J.; Yousufuddin, M.; Goddard III, W. A.; Periana, R. A. *Dalton Trans.* **2011**, *40*, 9094-9097.

(56) Ohanessian, G.; Goddard, W. A. *Acc. Chem. Res.* **1990**, *23*, 386-392.

(57) Tsay, C.; Livesay, B. N.; Ruelas, S.; Yang, J. Y. *J. Am. Chem. Soc.* **2015**, *137*, 14114-14121.

(58) Creutz, C.; Chou, M. H. *J. Am. Chem. Soc.* **2009**, *131*, 2794-2795.

(59) Pitman, C. L.; Brereton, K. R.; Miller, A. J. M. *J. Am. Chem. Soc.* **2016**, *138*, 2252-2260.

(60) Berning, D. E.; Miedaner, A.; Curtis, C. J.; Noll, B. C.; Rakowski DuBois, M. C.; DuBois, D. L. *Organometallics* **2001**, *20*, 1832-1839.

(61) Ciancanelli, R.; Noll, B. C.; DuBois, D. L.; DuBois, M. R. *J. Am. Chem. Soc.* **2002**, *124*, 2984-2992.

(62) Price, A. J.; Ciancanelli, R.; Noll, B. C.; Curtis, C. J.; DuBois, D. L.; DuBois, M. R. *Organometallics* **2002**, *21*, 4833-4839.

(63) Fong, H.; Peters, J. C. *Inorg. Chem.* **2015**, *54*, 5124-5135.

(64) Wayner, D. D. M.; Parker, V. D. *Acc. Chem. Res.* **1993**, *26*, 287-294.

(65) Connelly, S. J.; Wiedner, E. S.; Appel, A. M. *Dalton Trans.* **2015**, *44*, 5933-5938.

(66) Tissandier, M. D.; Cowen, K. A.; Feng, W. Y.; Gundlach, E.; Cohen, M. H.; Earhart, A. D.; Coe, J. V.; Tuttle, T. R. *J. Phys. Chem. A* **1998**, *102*, 7787-7794.

(67) Pegis, M. L.; Roberts, J. A. S.; Wasylenko, D. J.; Mader, E. A.; Appel, A. M.; Mayer, J. M. *Inorg. Chem.* **2015**, *54*, 11883-11888.

(68) Matsubara, Y.; Fujita, E.; Doherty, M. D.; Muckerman, J. T.; Creutz, C. *J. Am. Chem. Soc.* **2012**, *134*, 15743-15757.

(69) Marenich, A. V. K., C. P.; Thompson, J. D.; Hawkins, G. D.; Chambers, C. C.; Giesen, D. J.; Winget, P.; Cramer, C. J.; Truhlar, D. G.; Minnesota, U. o., Ed. Minneapolis, MN, 2012.

(70) Bourrez, M.; Molton, F.; Chardon-Noblat, S.; Deronzier, A. *Angew. Chem. Int. Ed.* **2011**, *50*, 9903-9906.